The interdependence of the kinematic and intrinsic parameters of a HIT cell: the effect of charge carrier mobility.

Abstract:

This paper discusses the dependence of the kinematic and intrinsic parameters of a silicon heterojunction solar cell, highlighting mobility phenomena.

First, a three-dimensional schematic of a HIT cell is established to highlight mobility phenomena at the texturized hydrogenated indium oxide (In_2O_3:H) contact layer and active layers where charge carriers move.

Next, mathematical equations linking the interacting physical parameters are developed, and the numerical resolution of these mathematical equations has led to results.

The discussion of these results is based on charge carrier transport, more specifically the photocurrent densities of free electrons and excitons, and their contribution in terms of the photovoltaic cell's energy production efficiency.

Introduction:

For several years, the photovoltaic industry has increasingly used semiconductors for the manufacture of solar cells. So far, most of these cells have been made of silicon, therefore, much research has been conducted on the physical properties of this material, in order to improve the processes of cell design and solar energy production.

Silicon properties depend on intrinsic and extrinsic parameters such as equilibrium concentrations, gap energy, diffusion and carrier mobility, all related to temperature. We give here the definition of these parameters and their dependence on temperature, often obtained empirically. The interaction of these parameters will be described by a color code that defines a system of two physical phenomena that we will have to explain.

Since mobilities are linked together through temperature, we will first combine them with temperature to see their effects on photocurrent densities before making them interact with photocurrent densities and internal quantum yields. So to better understand the contribution of mobility on the efficiency of the cell to produce energy, a study of the influence of temperature on the mobilities of load carriers is required.

1. Demonstrating mobility phenomena in a silicon heterojunction cell

The texturing operation aims to develop a micrometric relief on the surface, enabling multiple reflections to reduce the cell's reflectivity. This reduction in reflectivity improves the probability of photon absorption at the surface of the silicon heterojunction cell or high efficiency cell (HIT).

Transparent conductive oxides (TCOs) have a high gap and are in fact degenerate semiconductors. In addition, the high gap of TCOs, between 3 and 4 eV [1,2,3], prevents them from absorbing photons with energies lower than the gap, making them transparent to visible and infrared light.

Incorporating hydrogen into zinc oxide (ZnO:H) and indium oxide (In_2O_3:H) TCOs is an effective technique for improving charge carrier mobility [4]. It reduces the transparency-conductivity trade-off within thin films [5].

This mobility enhancement in sputtered ZnO:H films reaches 47.1 $cm^2.V^{-1}.s^{-1}$ for a carrier concentration of 4.4×10^{19} cm^{-3} [6]. Mobility values in excess of 100 $cm^2.V^{-1}.s^{-1}$ can be achieved with a charge carrier concentration approaching 10^{20} cm^{-3} in In_2O_3:H films [7,8,9].

As a result, materials with higher mobility than tin-doped In_2O_3 (Indium Tin Oxide or ITO) are being successfully implemented in silicon (Si) heterojunctions, following the success of In_2O_3:H . To achieve low parasitic absorption and high conductivity, the top electrode must have a relatively low carrier density, but high mobility. [10,11,12]

In_2O_3:H is a high-mobility TCO material with superior transmittance in the visible and near infrared [5], and excellent thermal and chemical stability for solar cell applications [13,14].

Thus, in our study we can take into account the excitons that can be excited with infrared light using the In_2O_3:H on solar cells as a front contact. Where light passes through in order to reach the active layers of the photovoltaic cell. In the case of amorphous or crystalline silicon thin-film solar cells, the light-scattering ability of the TCOs comes into play.

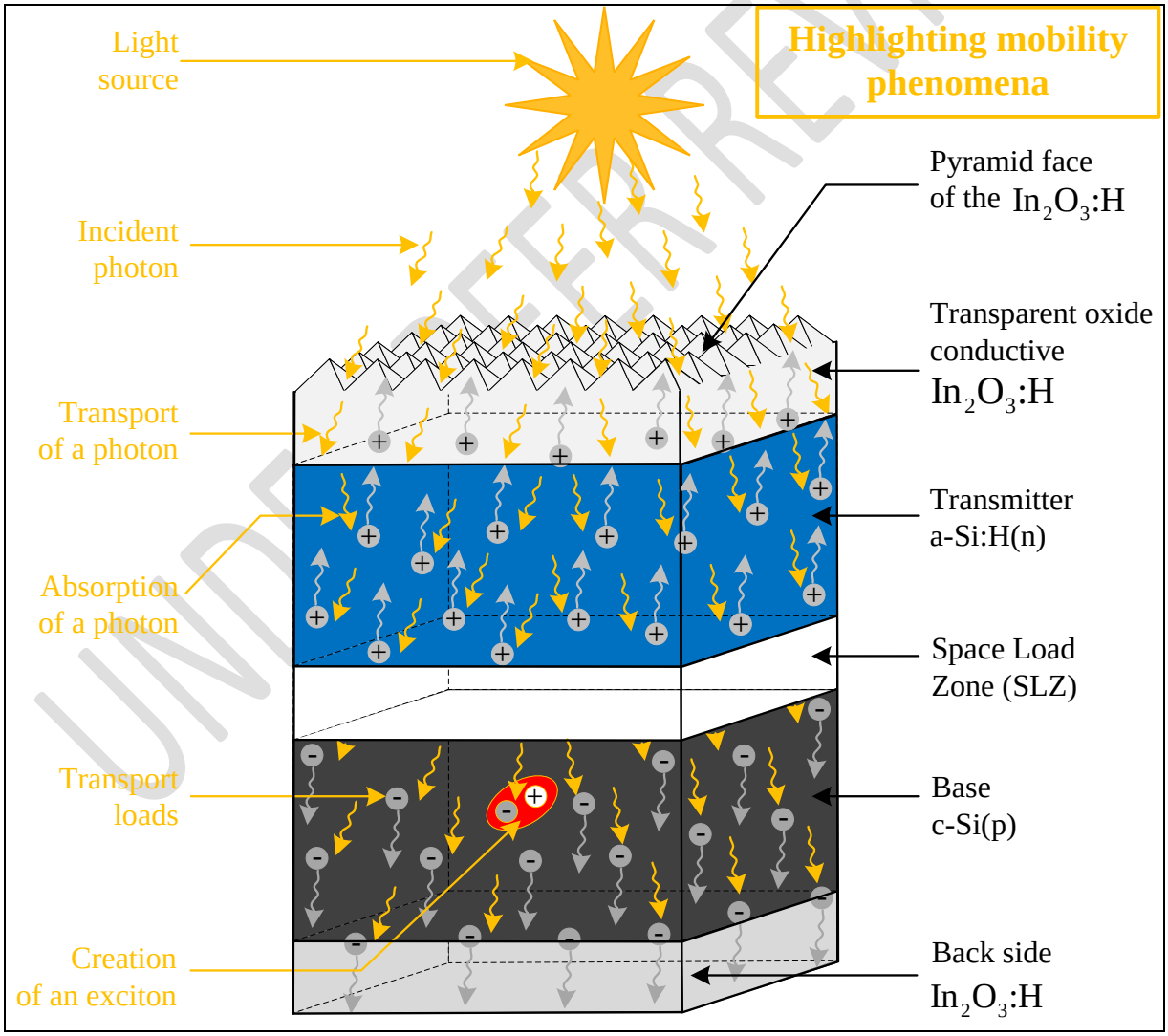

Figure 1: Mechanisms of carrier mobility in a sunlit silicon heterojunction cell.

The emitter, doped with donor atoms, has positively-charged holes as minority carriers, while the base, doped with acceptor atoms, has negatively-charged electrons as minority carriers. The emitter and base are the active layers of the HIT cell, where the minority charge carriers are created.

These active layers are separated by a charge-free zone where an electric field prevails due to a potential difference. In the presence of photon energy, the minority charge carriers move through mechanisms of transition from one band to another, separation and propagation towards the receiving electrodes (anode and cathode) with the help of the electric field in the depletion zone.

These propagation or generation mechanisms are more complex with excitons, as the charge carriers in this hydrogenoid complex are linked by an attractive or Coulombic force. Their movement is conditioned by multiphonon and interband relaxations, often leading to annihilation phenomena before being dissociated and recombined.

Since the physical phenomena are interrelated, the electric field of the space charge zone diffuses the minority charge carriers, leading to their mobility. To model these physical phenomena, we have used mathematical equations to express the dependence of kinematic and intrinsic parameters.

2. Expressions of some intrinsic and kinematic parameters

2.1 Intrinsic parameters

The electronic properties of crystalline silicon depend on intrinsic parameters such as equilibrium free-carrier concentrations, gap energy and the presence of impurities. These parameters are temperature-dependent. Here, we define these parameters and show their dependence on temperature, often obtained empirically.

Equilibrium carrier densities (n_{0e} for electrons, n_{0h} for holes) are given by the following expressions:

$$n_{0e}(T) = n_C \times e^{-\frac{(E_C - E_F)}{kT}} \quad \text{and} \quad n_{0h}(T) = n_V \times e^{-\frac{(E_F - E_V)}{kT}}$$

With n_C and n_V the respective densities of states of the conduction and valence bands, and E_F the Fermi energy level.

The values of n_C and n_V are often given as $n_C \approx 3\times10^{19}$ cm^{-3} and $n_V \approx 1\times10^{19}$ cm^{-3} respectively at 300 K [15]. In fact, a parameterization taking into account the evolution of effective masses with temperature between 200 K and 500 K was given by Green [16]:

$$n_C(T) = 3\times10^{19} \times \left(\frac{T}{300}\right)^{1.5} \quad \text{et} \quad n_V(T) = 1\times10^{19} \times \left(\frac{T}{300}\right)^{1.5}$$

We can base this on the intrinsic density of state, which in addition to being a function of temperature (T), is also expressed as a function of the gap energy (E_g), which is an energy difference between the valence band and the conduction band, of respective density of state n_V and n_C. Hence the product $n_{0e} \times n_{0h}$, which defines the intrinsic carrier density:

$$n_i(T) = \sqrt{n_{0e} \times n_{0h}}$$

Taking the above into account, the intrinsic carrier density is then rewritten as:

$$n_i(T) = (n_C \times n_V)^{0.5} \times e^{-\left(\frac{E_g(T)}{2\times V_T}\right)}$$

Where A is the thermal potential defined as:

$$V_T = \frac{k_b \times T}{q}$$

And E_g the temperature-dependent gap energy, described by several empirical models developed since the 60s [17]. The most common model is that given by Varshni (with Thurmond coefficients) [18,19], corroborated more recently by photoluminescence measurements [20], and valid up to temperatures above 750 K:

$$E_g(T) = E_g(0) - \frac{\delta \times T^2}{T - \beta}$$

Gap energy depends on the intrinsic parameters β and δ of the material used. For silicon, we obtain a value for $\beta = 636 \pm 50$ K and a value for $\delta = 4{,}73 \times 10^{-4}$ eV.K^{-1}.

Intrinsic parameters play a key role in the conversion of photon energy into electrical energy, through the ordered movement of charged electrons, which is facilitated by the crystallographic structure of silicon. Silicon in its intrinsic state, without any external influence, behaves like an insulator and doesn't allow electrons to move. But in the presence of a few extrinsic parameters: temperature, doping and $h\nu$ -energy photons, it becomes not only a conductor of energy, but also a producer of electricity.

2.2 Kinematic parameters

In addition to intrinsic parameters, there are extrinsic parameters such as doping levels, which give rise to a potential difference V_b that depends on the thermal potential V_T, the intrinsic density of state n_i and the doping levels of acceptors N_A and donors N_D.

$$V_b = V_T \times \ln\left(\frac{N_A \times N_D}{n_i^2}\right)$$

This internal potential leads to an electric field $\vec{E}$, which allows charge carriers to diffuse into the material.

Since the study focuses on two types of charge carriers, free electrons and excitons, we have defined the diffusion coefficients of free electrons D_e and excitons D_x as follows:

$$D_e = V_T \times \left[86.5 + 1268\left(1 + \frac{N_A}{7.7 \times 10^{18}}\right)^{-0.91} - \left(\frac{1.4 \times 10^{19}}{N_A}\right)\right] \times \left(\frac{T}{300}\right)^2 \quad \text{and} \quad D_x = \frac{300}{T^{0.5}}$$

From the charge carrier diffusion coefficients we deduce the mobility coefficients.

The mobility of free carriers in silicon has been measured mainly by the Hall effect [21] and by high-speed and high-frequency devices [22]. Empirical [23,24,25,26] and analytical formulations have been proposed as a function of doping atom density (As, P or B) and temperature. The most widely used formulation for doping dependence is that of Masetti et al. [26], valid in the following doping density intervals (cm^{-3}): $\left[10^{13}\ ,\ 5 \times 10^{21}\right]$ and $\left[10^{14}\ ,\ 1{,}2 \times 10^{21}\right]$ for phosphorus and boron respectively.

Charge carrier mobility ($\mu_{e,x}$) depends on the material's intrinsic parameters. The latter, together with external parameters [27,28], condition the movement of charge carriers in a photovoltaic cell.

$$\mu_{e,x}(T) = \frac{D_{e,x}}{V_T}$$

This kinematic parameter plays a key role in the dependence of kinematic and intrinsic parameters on solar cell performance.

3. Dependence of photocurrent densities on electron and exciton mobilities

Since mobilities are linked to each other via temperature, we'll first combine them with temperature to see their effects on photocurrent densities and internal quantum yields. So, to better understand the effect of temperature on charge carrier mobilities, a study of the influence of temperature is in order.

3.1. The effect of temperature on charge carrier mobility

An increase in temperature leads to a decrease in exciton mobility and an increase in electron mobility. The simultaneous variation in carrier mobility as a function of temperature is defined by a color code.

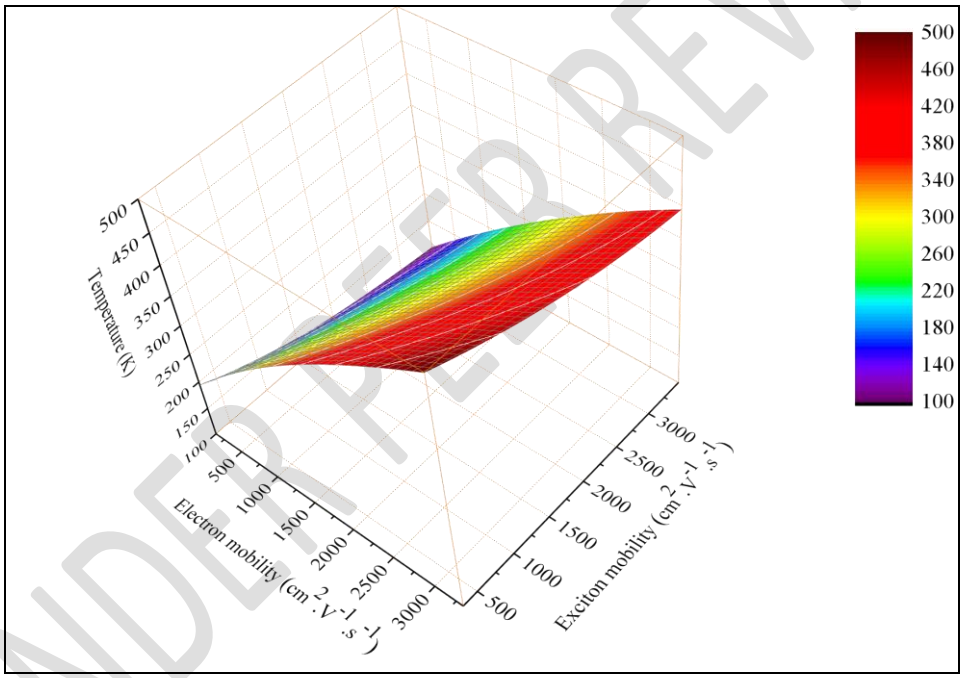

Figure 2: The simultaneous influence of temperature on the mobility of free and bound charge carriers (excitons)

The antagonistic phenomena of free electron and exciton mobilities with respect to temperature are observed, and they compensate each other in a balanced way with respect to temperature. Variations in charge carrier mobility are governed by a thermal energy source that enables the cell to conserve photogenerated energy.

3.2. The simultaneous effect of temperature and electron mobility on electron photocurrent density

Figure 3 shows the photocurrent density of electrons as a function of temperature and electron mobility.

We obtain low photocurrent densities (below $6.27\ \mathrm{mA.cm^{-2}}$) at temperatures below 250 K whatever the electron mobility between 250 and $3500\ \mathrm{cm^2.V^{-1}.s^{-1}}$. Above a temperature of 250 K, electron

photocurrent density increases progressively to $22.30\ \mathrm{mA.cm^{-2}}$ for electron mobilities between 1000 and $2000\ \mathrm{cm^2.V^{-1}.s^{-1}}$.

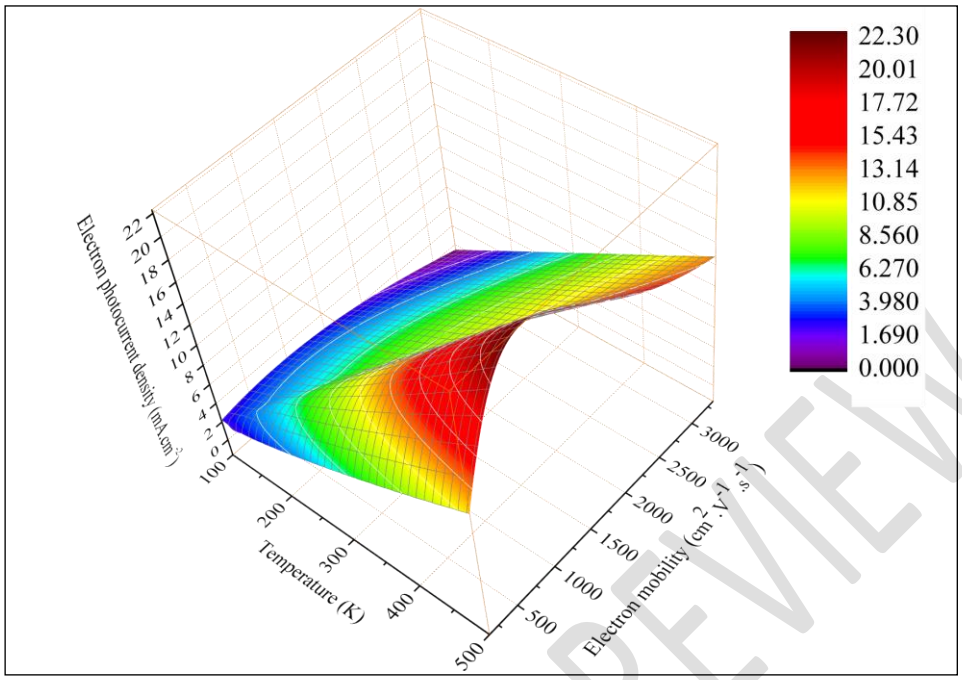

Figure 3: Electron photocurrent density as a function of temperature and electron mobility

The excitatory effect of temperature on semiconductor electrons promotes the orderly movement of charge carriers, but not more than the mobility of free electrons. This mobility, although facilitated by temperature, has a more consequential influence on photocurrent density at values around $1000\ \mathrm{cm^2.V^{-1}.s^{-1}}$ where we obtain the maximum photocurrent density of electrons.

Mobilities below $500\ \mathrm{cm^2.V^{-1}.s^{-1}}$ coincide with low temperatures, synonymous with inactivation of the cell's electronic structure. Whereas mobilities above $1500\ \mathrm{cm^2.V^{-1}.s^{-1}}$ coincide with high temperatures, synonymous with disorder in the cell's electronic structure.

As a result, we don't have to grope to see which mobility value is more suitable to get the maximum photogenerated free carriers.

Excitons often behave in the opposite way to free charge carriers in certain physical phenomena. Following on from our work, we have developed a study of the simultaneous effect of temperature and exciton mobility on exciton photocurrent density.

3.3 The simultaneous effect of temperature and exciton mobility on exciton photocurrent density

In Figure 4, for exciton mobilities ranging from 250 to $2500\ \mathrm{cm^2.V^{-1}.s^{-1}}$ and temperatures between 250 K and 500 K, we observe exciton photocurrent densities below $1.322\ \mathrm{Ma.cm^{-2}}$. At temperature values below 250 K or very low around 100 K, we observe a slight increase in exciton photocurrent density up to $1.37\ \mathrm{mA.cm^{-2}}$ and a maximum peak of $1.433\ \mathrm{mA.cm^{-2}}$ at exciton mobilities above $3000\ \mathrm{cm^2.V^{-1}.s^{-1}}$.

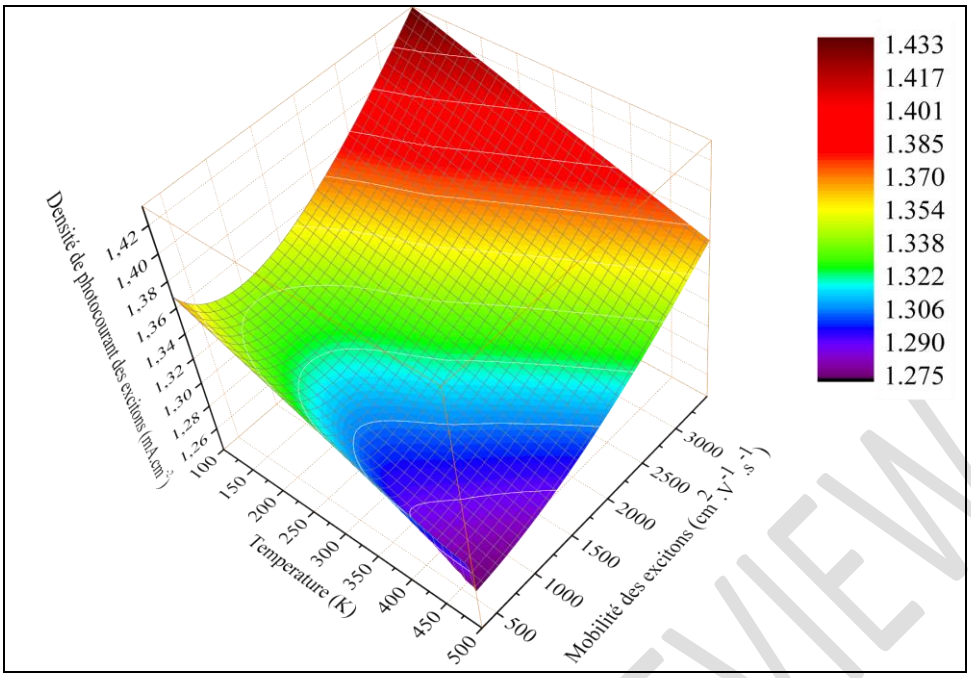

Figure 4: Exciton photocurrent density as a function of temperature and exciton mobility

The excitatory effect of temperature on the semiconductor excitons disfavors the ordered movement of excitons, but no more than the mobility of excitons. This mobility, although facilitated by temperature, adversely affects the photocurrent density at values around $1000\ \mathrm{cm^2.V^{-1}.s^{-1}}$ where we obtain the minimum photocurrent density of excitons. Hence the antagonistic phenomenon of mobility on the photocurrent densities of free electrons and that of excitons.

We're not looking for the maximum number of excitons photogenerated in the cell, but above all the maximum number of charge carriers photogenerated. If we keep temperatures low to obtain the maximum number of photogenerated excitons, we risk a drastic loss of photogenerated free electrons of $20.0\ \mathrm{mA.cm^{-2}}$ for a small gain in photogenerated excitons of $0.079\ \mathrm{mA.cm^{-2}}$. This study is therefore designed to obtain the maximum photocurrent density of charge carriers at suitable mobilities.

We will also study the interdependence between photocurrent densities, electron mobilities and exciton mobilities.

3.4. The simultaneous effect of electron and exciton mobilities on electron photocurrent density

Figure 5 shows the photocurrent density of electrons as a function of the respective electron and exciton mobilities.

Whatever the mobility value between 500 and $3500\ \mathrm{cm^2.V^{-1}.s^{-1}}$, the electron photocurrent density exceeds $8.0\ \mathrm{mA.cm^{-2}}$ and can approach $13.0\ \mathrm{mA.cm^{-2}}$ at exciton mobilities below $500\ \mathrm{cm^2.V^{-1}.s^{-1}}$. We also noticed a decrease in electron photocurrent density as exciton mobility increased.

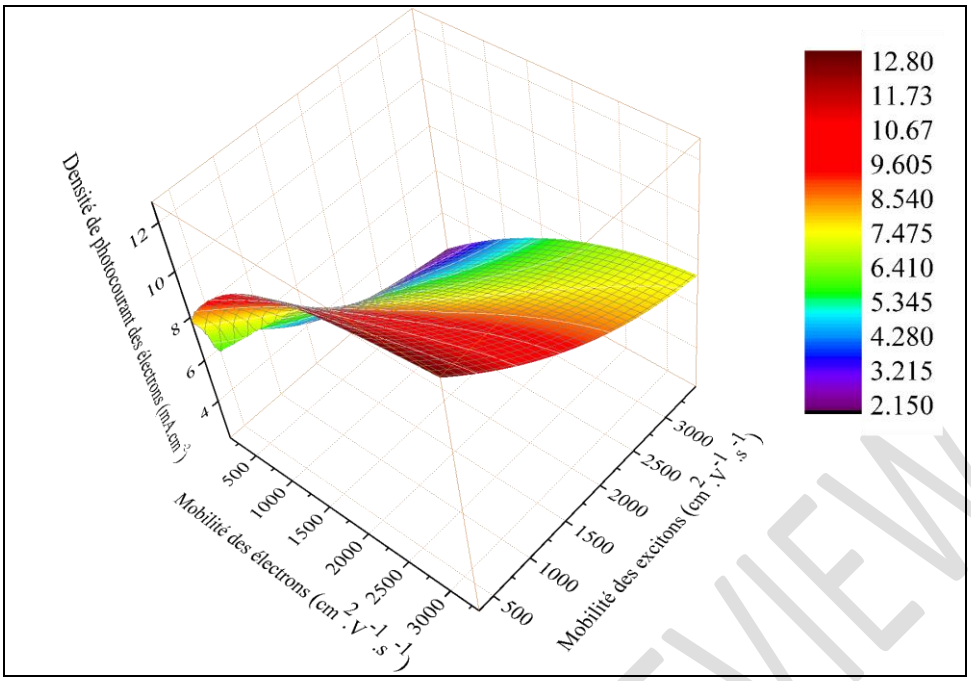

Figure 5: Electron photocurrent density as a function of electron and exciton mobility

For charge carrier mobility to be beneficial to electron photocurrent density, free charge carriers must be more mobile and excitons less mobile. High mobility of free electrons enables them to photogenerate as quickly as possible, minimizing recombination. This mobility, facilitated by temperature, is partly due to the electric field in the depletion zone and partly to the photon energy allocated to them by a light source. In addition, high electron mobility is synonymous with energy conservation, as this increasing mobility is due to a source of thermal energy. In addition, this conservation of photon energy must be accompanied by stability of the semiconductor structure. This stability is controlled by the low mobility of the excitons.

As we have seen in Figure 2, the antagonistic character of charge carrier mobilities on electron photocurrent density is observed. In other words, the lowest values of electron photocurrent density are obtained at very low values of electron mobility and very high exciton mobilities. This simultaneous influence of mobilities on electron photocurrent density is balanced. This is not the case for exciton photocurrent density.

3.5. The simultaneous effect of electron and exciton mobilities on exciton photocurrent density

Furthermore, we found in Figure 6 that the exciton photocurrent density reaches a maximum peak of $2.22\ \mathrm{Ma.cm^{-2}}$ with free electron and exciton mobilities below $1000\ \mathrm{cm^2.V^{-1}.s^{-1}}$. We also noted a slight increase in photocurrent density, relative to exciton mobility from a value of $1.27\ \mathrm{mA.cm^{-2}}$ to a value of $1.46\ \mathrm{mA.cm^{-2}}$.

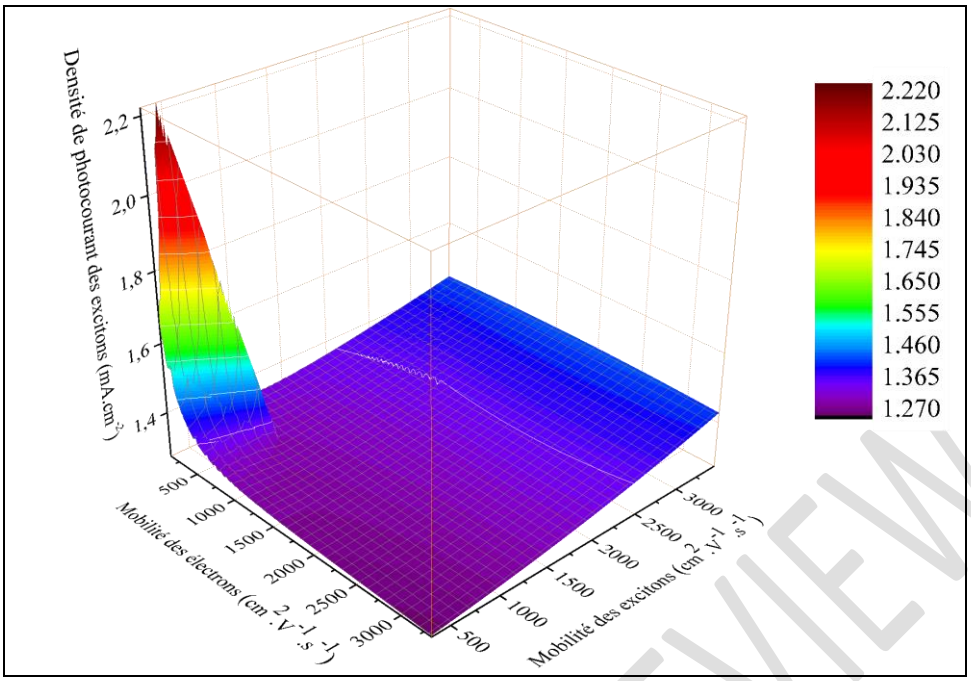

Figure 6: Exciton photocurrent density as a function of electron and exciton mobility

When free electrons lose their mobility, they are able to relax to excited levels, contributing a surplus to the excitons already present in the cell. This contribution, shown in Figure 6, is greater than that of the excitons, which increases with their mobility. The excitonic quantities studied therefore provide a surplus of exciton photocurrent densities, acting as energy conservers through a process of intra-band relaxation of free electron-hole pairs. This enables us to conserve some of the photogenerated energy in poor weather conditions. This excitonic phenomenon may also explain the low currents observed in the dark.

It's good to know how and by how much charge carriers are photogenerated. But it's even better to know how much energy photovoltaic cells produce. And the quantum efficiency of charge carriers gives us an insight into this energy contribution. Since we have two types of charge carrier, it's a good idea to study the contribution of each and deduce their utility.

3.6. The behavior of the internal quantum yield of charge carriers on the physical parameters studied

Consequently, whatever the temperature or electron mobility, associated with exciton mobility below 1000 $cm^2.V^{-1}.s^{-1}$, we obtain charge carrier internal quantum yields between 50 and 76.8 %. These internal charge carrier quantum yields are shown in Figures 7 and 8.

Whether it's temperature or electron mobility, we obtain better quantum yields than when associating them with low exciton mobilities. We can therefore state that exciton mobility is an excitonic phenomenon that adversely affects charge carrier internal quantum yields, in contrast to free electron mobility, which leads to internal quantum yields in excess of 50 %.

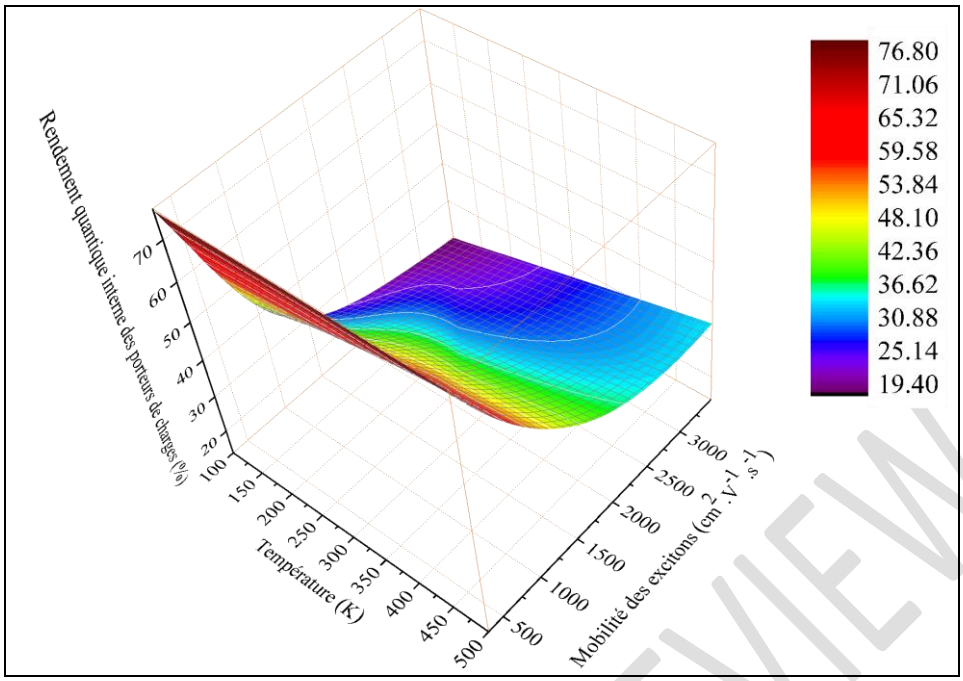

Figure 7: Internal quantum yield of charge carriers as a function of temperature and exciton mobility

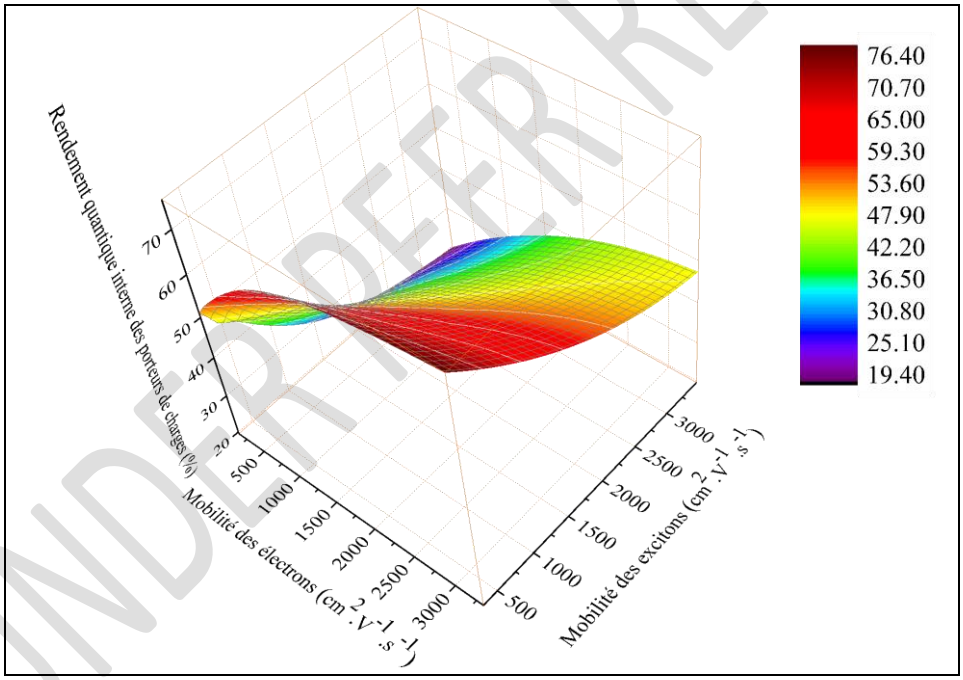

Figure 8: The internal quantum yield of charge carriers as a function of electron and exciton mobility.

So we can by making these types of cell avoided having exciton mobility values that exceed $1000\ \mathrm{cm^2.V^{-1}.s^{-1}}$ to have maximum charge carrier internal quantum efficiency and good photovoltaic energy production from the HIT cell.

Conclusion:

Variations in charge carrier mobilities are governed by a thermal energy source that enables the cell to conserve the energy photogenerated by free charge carriers and excitons. The excitonic quantities studied not only allow us to have a surplus of exciton photocurrent densities, they also play a role in energy conservation through an intra-band relaxation process of free electron-hole pairs. This enables

us to conserve some of the photogenerated energy in poor weather conditions. This excitonic phenomenon may also explain the low currents observed in the dark.

We're not looking for the maximum number of excitons photogenerated in the cell, but rather the maximum number of charge carriers photogenerated. If we keep temperatures low to obtain the maximum number of photogenerated excitons, we risk a drastic loss of photogenerated free electrons of $20.0\ \mathrm{mA.cm^{-2}}$ for a small gain in photogenerated excitons of $0.079\ \mathrm{mA.cm^{-2}}$. So this study is also designed to obtain the maximum photocurrent density of charge carriers at suitable temperatures.

So we can when fabricating these types of cell take into account exciton mobility values around $1000\ \mathrm{cm^2.V^{-1}.s^{-1}}$ to have internal charge carrier quantum efficiencies approaching 70 % and good photovoltaic energy production from the HIT cell.

References:

[1]. Hiroshi Yanagi, Hiroshi Kawazoe, Atsushi Kudo, Masahiro Yasukawa and Hideo Hosono. Chemical Design and Thin Film Preparation of p-Type Conductive Transparent Oxides. Journal of Electroceramics 4 (2/3), 407-414, 2000.

[2]. Xiliang Nie, Su-Haï Wei, and S. B. Zhang. Bipolar Doping and Band-Gap Anomalies in Delafossite Transparent Conductive Oxides. Physical Review Letters 88 (6), 066405(1-4), 2002.

[3]. Yu Yang, Shu Jin, Julia E. Medvedeva, John R. Ireland, Andrew W. Metz, Jun Ni, Mark C. Hersam, Arthur J. Freeman, and Tobin J. Marks. Journal American Chemical Society 127 (24), 8796-8804, 2005.

[4]. Leonard Tutsch, Frank Feldmann, Bart Macco, Martin Bivour, Erwin Kessels, and Martin Hermle. Improved Passivation of n-Type Poly-Si Based Passivating Contacts by the Application of Hydrogen-Rich Transparent Conductive Oxides. IEEE Journal of Photovoltaics 10 (4), 986-991, 2020.

[5]. Takashi Koida, Hiroyuki Fujiwara, and Michio Kondo. Hydrogen-doped In_2O_3 as high-mobility transparent conductive oxide, Japanese Journal of Applied Physics 46 (28), 685-687, 2007.

[6]. D. Gaspar, L. Pereira, K. Gehrke, B. Galler, E. Fortunato, R. Martins. Solar Energy Materials & Solar Cells 163, 255-262, 2017.

[7]. Takashi Koida, Hiroyuki Fujiwara, and Michio Kondo. Structural and electrical properties of hydrogen-doped In_2O_3 films fabricated by solid-phase crystallization. Journal of Non-Crystalline Solids 354 (19), 2805-2808, 2008.

[8]. Barraud L, Holman ZC, Badel N, Reiss P, Descoeudres A, Battaglia C, De Wolf S, Ballif C. Hydrogen-doped indium oxide/indium tin oxide bilayers for high-efficiency silicon heterojunction solar cells. Solar Energy Materials and Solar Cells 115, 151-156, 2013.

[9]. Wardenga HF, Frischbier MV, Morales-Masis M, Klein A. In Situ Hall Effect Monitoring of Vacuum Annealing of In_2O_3 : H Thin Films. Materials 8(2), 561-574, 2013.

[10]. Yuqiang Liu, Yajuan Li, Yiliang Wu, Guangtao Yang, Luana Mazzarella, Paul Procel-Moya, Adele C. Tamboli, Klaus Weber, Mathieu Boccard, Olindo Isabella, Xinbo Yang and Baoquan Sun. High-Efficiency Silicon Heterojunction Solar Cells: Materials, Devices and Applications. Materials Science & Engineering R 142, 1-116, 2020.

[11]. Takashi Koida, Hiroyuki Fujiwara, and Michio Kondo. High-mobility hydrogen-doped In_2O_3 transparent conductive oxide for a-Si:H/c-Si heterojunction solar cells. Solar Energy Materials and Solar Cells 93(6), 851-854, 2009.

[12]. L. Barraud, Z.C. Holman, N. Badel, P. Reiss, A. Descoeudres, C. Battaglia, S. De Wolf, C. Ballif. Hydrogen-doped indium oxide/indium tin oxide bilayers for high-efficiency silicon heterojunction solar cells. Solar Energy Materials and Solar Cells 115, 151-156, 2013.

[13]. Timo Jäger, Yaroslav E. Romanyuk, Shiro Nishiwaki, Benjamin Bissig, Fabian Pianezzi, Peter Fuchs, Christina Gretener, Max Döbeli, and Ayodhya N. Tiwari. Hydrogenated indium oxide window layers for high-efficiency $Cu(In,Ga)Se_2$ solar cells. Journal of Applied Physics 117 (20), 5301(1-7), 2015.

[14]. Fan Fu, Thomas Feurer, Timo Jäger, Enrico Avancini, Benjamin Bissig, Songhak Yoon, Stephan Buecheler and Ayodhya N. Tiwari. Low-temperature-processed efficient semi-transparent planar perovskite solar cells for bifacial and tandem applications 18 (6), 8932(1-9), 2015.

[15]. Rebert W. Miles, Kathleen M. Hynes and Ian Forbes. Photovoltaic solar cells: An overview of state-of-the-art cell development and environmental issues. Progress in Crystal Growth and Characterization of Materials 51 (1-3), 1-42, 2005.

[16]. Martin A. Green. Intrinsic concentration, effective densities of states, and effective mass in silicon. Journal of Applied Physics 67 (6), 2944-2954, 1990.

[17]. Rudi C. Vankemmel, Wim Schoenmaker and Kristin M. de Meyer. A unified wide temperature rande model for the energy gap, the effective carrier mass and intrinsic concentration in silicon. Solid-State Electronics 36 (10), 1379-1384, 1993.

[18]. Yatendra Pal Varshni. Temperature dependence of the energy gap in semiconductors. Physica 34 (1), 149-154, 1967.

[19]. C. D. Thurmond. The Standard Thermodynamic Functions for the Formation of Electrons and Holes in Ge, Si, GaAs, and GaP. Journal of The Electrochemical Society 122 (8), 1133-1141, 1975.

[20]. V. Alex, S. Finkbeiner and J. Weber. Temperature dependence of the indirect energy gap in crystalline silicon. Journal of Applied Physics 79 (9), 6943-6946, 1996.

[21]. A. Sproul et M. Green. Improved value for the silicon from 275 to 375 K. Journal of Applied Physics 70 (2), 846-854, 1991.

[22]. P. Norton, T. Braggins and H. Levinstein. Impurity and Lattice Scattering Parameters as Determined from Hall and Mobility Analysis in n-Type Silicon. Physical Review 8 (12), p. 5632-5653, 1973.

[23]. C. Canali, C. Jacoboni, G. Ottaviani, and A. Alberigi-Quaranta. High-field diffusion of electrons in silicon. Quaranta Applied Physics Letters 27 (5), 278-280, 1975.

[24]. Carlo. Jacoboni, Claudio. Canali, Giampioro P. Otiaviani et Alessandro Alberigi-Quaranta. A review of some charge transport properties of silicon. Solid-State Electronics 20 (2), 77-89, 1977.

[25]. Shengsan Li and Rebert W. Thurber. The dopant density and temperature dependence of electron mobility and resistivity in n-type silicon. Solid-State Electronics 20 (7), 609-616, 1977.

[26]. G. Masetti, M. Severi and S. Solmi. Modeling of carrier mobility against carrier concentration in arsenic-, phosphorus-, and boron-doped silicon. IEEE Transactions on Electron Devices 30 (7), 764-769, 1983.

[27]. Dirk B. M. Klaassen. A unified mobility model for device simulation-I. model equations and concentration dependence. Solid-State Electronics 35 (7), 953-959, 1992.

[28]. Dirk B. M. Klaassen. A unified mobility model for device simulation-II. Temperature dependence of carrier mobility and lifetime. Solid-State Electronics 35 (7), 961-967, 1992.